APL Photonics

On the observation of dispersion in tunable second-order nonlinearities of silicon-rich nitride thin films

Cite as: APL Photonics 4, 036101 (2019); https://doi.org/10.1063/1.5053704
Submitted: 24 August 2018 . Accepted: 11 February 2019 . Published Online: 05 March 2019

Hung-Hsi Lin, Rajat Sharma, Alex Friedman, Benjamin M. Cromey, Felipe Vallini, Matthew W. Puckett, Khanh Kieu, and Yeshaiahu Fainman

On the observation of dispersion in tunable second-order nonlinearities of silicon-rich nitride thin films

Cite as: APL Photon. 4, 036101 (2019); doi: 10.1063/1.5053704
Submitted: 24 August 2018 • Accepted: 11 February 2019 •
Published Online: 5 March 2019

Hung-Hsi Lin,[1,a)] Rajat Sharma,[2,a),b)] Alex Friedman,[2] Benjamin M. Cromey,[3] Felipe Vallini,[2] Matthew W. Puckett,[2] Khanh Kieu,[3] and Yeshaiahu Fainman[2]

AFFILIATIONS

[1]Materials Science and Engineering, University of California, 9500 Gilman Drive, La Jolla, San Diego, California 92093, USA
[2]Department of Electrical and Computer Engineering, University of California, 9500 Gilman Drive, La Jolla, San Diego, California 92093, USA
[3]College of Optical Sciences, The University of Arizona, 1630 E University Blvd., Tucson, Arizona 85719, USA

[a)]**Contributions:** H.-H. Lin and R. Sharma contributed equally to this work.
[b)]**Author to whom correspondence should be addressed:** r8sharma@eng.ucsd.edu

ABSTRACT

We present experimental results on second-harmonic generation in non-stoichiometric, silicon-rich nitride films. The as-deposited film presents a second-order nonlinear coefficient, or $\chi^{(2)}$, as high as 8 pm/V. This value can be widely tuned using the electric field induced second harmonic effect, and a maximum value of 22.7 pm/V was achieved with this technique. We further illustrate that the second-order nonlinear coefficient exhibited by these films can be highly dispersive in nature and require further study and analysis to evaluate their viability for in-waveguide applications at telecommunication wavelengths.

INTRODUCTION

There is an acute need for a highly nonlinear material that can be integrated with silicon to achieve efficient, high-speed, linear electro-optic modulation, and nonlinear wave mixing.[1–3] In recent years, silicon nitride has emerged as one such promising candidate with salient features such as a wide transparency window, ease of fabrication and compatibility with silicon photonics manufacturing.[4] While traditionally silicon nitride has been seen as a centrosymmetric dielectric, lacking any second-order nonlinear susceptibility,[5] recent results in the literature have shown that silicon nitride can exhibit an anomalous second-order nonlinear susceptibility,[6,7] the origin of which remains unclear.

While reported results have shown the second-order nonlinear properties of silicon nitride thin-films to vary across deposition techniques and associated conditions, work in the literature has not focused on the variety of wavelengths employed in these experimental studies. There have been reports in the literature on thin-films of stoichiometric silicon nitride which have demonstrated a bulk second-order nonlinear susceptibility, $\chi^{(2)}$, as high as ~3 pm/V, at a pump wavelength of 800 nm;[6,7] while other results have utilized in-waveguide, phase-matched, second harmonic generation (SHG) to report values as low as ~0.3 pm/V in stoichiometric films at a pump wavelength of 1550 nm.[7,8] Previously, the authors have attributed this discrepancy, in measured coefficients using free-space and in-waveguide measurements, to a lack of perfect phase-matching and/or modifications introduced into the materials during fabrication.[7] To the best of our knowledge, there has not been a conclusive discussion or reported results thus far on this discrepancy, and its dispersive nature, in the literature.

In this manuscript, we undertake a systematic evaluation of the second-order nonlinear properties exhibited by silicon nitride thin films. We discuss methods to enhance the observed $\chi^{(2)}$ by both increasing the silicon content in the films as well as through the electric-field induced second-harmonic effect (EFISH). Finally, we also report on our observation of a high degree of dispersion in the $\chi^{(2)}$ exhibited by these films.

SILICON-RICH NITRIDE

Bulk nonlinearities in silicon nitride thin films deposited through plasma enhanced chemical vapor deposition, PECVD, and RF magnetron sputtering have been reported on in the past.[6] The first measurement of this nonlinearity using in-waveguide experiments was reported in 2016,[7] where the authors carried out phase-matched second-harmonic generation in stoichiometric silicon nitride waveguides. The magnitude of the reported nonlinearity was low with in-waveguide measurements (at 1550 nm) yielding values of $\chi^{(2)}$ lower than 1 pm/V. These values have subsequently been reproduced and confirmed in a separate measurement by Billat *et al.*[8] By leveraging a unique attribute of the silicon nitride platform, this relatively small nonlinearity can be enhanced by changing the stoichiometry of the deposited films. It is known that increasing the silicon content in sputtered silicon nitride thin films, yielding the so-called silicon-rich nitride (SRN) films, leads to an enhancement in the magnitude of the third-order nonlinearity.[9] However, these films suffer from high propagation loss, making them inapplicable to many in-waveguide applications. There have been two recent reports[10,11] extending these results to PECVD deposited SRN films carried out using free-space measurements with pump wavelengths of 800 nm and 1040 nm, respectively. The SRN material was shown to possess an enhanced second-order nonlinearity compared to that of stoichiometric films, while its propagation loss values remained relatively low.

With an intent to evaluate these films for in-waveguide applications, we carried out a systematic study of the effect of silicon content on the exhibited linear and nonlinear optical properties of the films. Three different samples, labeled S_1, S_2, and S_3, were fabricated with silicon nitride films deposited on fused-silica substrates. The flow-rate of silane (SiH_4), one of the precursors in the PECVD process, was varied across the samples from 180, 276, and 500sccm, while keeping all the other deposition parameters (outlined in Ref. 7) constant. Ellipsometry measurements using light at 632.8 nm confirmed that this fabrication process produced films with unequal refractive indices of 1.9 (S_1), 2.08 (S_2), and 2.25 (S_3), with the index of the film scaling positively with the SiH_4 flow-rate. The reason for this was confirmed to be an increase in silicon content by carrying out electron-dispersive X-ray (EDX) spectroscopic measurements. Figure 1(a) shows the composition of the films in terms of their silicon and nitride atomic percentages (shown in red and blue arrows, respectively), with a silicon content of 41% (S_1), 51% (S_2), and 56% (S_3) across the three films.

FREE-SPACE MEASUREMENTS

In order to characterize the effect of the silicon content in these films on their nonlinear properties, polarization dependent SHG experiments were carried out using a femtosecond Ti:Sapphire laser source at a wavelength of 800 nm, with a pulse duration of 150 fs, an 80 MHz repetition rate, and a 100 mW of average power. The pump beam was focused using a 20× microscope objective to a focal spot on the surface of the SRN sample, with a beam waist of 50 μm and a confocal parameter much longer than the thickness of the film. The generated s- and p-polarized SHG signals were detected as a function of the polarization angle of the pump. Further details of the characterization setup can be found in the supplementary material. All of the SiN thin films were grown to the same thickness of 400 nm and were deposited on 1.5 cm × 1.5 cm fused silica

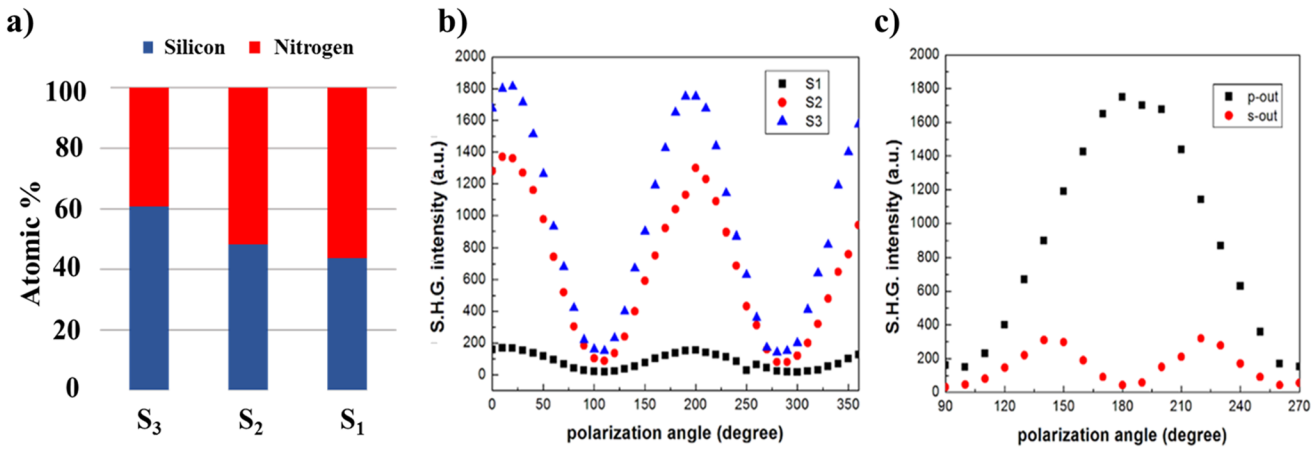

FIG. 1. (a) Composition of the samples, S_1, S_2, and S_3, in terms of the atomic percentages of silicon and nitrogen, extracted using EDX spectroscopy. (b) Second-harmonic signals generated from the three films as a function of polarization angle for p-polarization. (c) SHG signals from the SRN film (S_3) for both s- and p-polarized input pumps.

TABLE I. The deposition recipes and measured properties of silicon nitride thin films.

Sample	SiH_4 flow rate (sccm)	Si (%)	Refractive index (λ = 632.8 nm)	$\chi^{(2)}_{zzz}$ (pm/V)	$\chi^{(2)}_{zxx}$ (pm/V)
S_1	180	41	1.9	2.4	0.4
S_2	276	51	2.08	5.8	1.1
S_3	500	56	2.25	8	1.9

substrates. A commercial 500 μm thick X-cut quartz wafer, exhibiting a nonlinear coefficient $\chi^{(2)}_{xxx}$ of 0.64% ± 8% pm/V is used to calibrate the system, and the absolute values of $\chi^{(2)}$ tensor components from our samples are determined by comparing the generated SHG signals with those from the quartz sample under the same experimental conditions. The use of thin-films in this study helps to avoid the need for any phase-matching, including the need to account for dispersion in the linear refractive index in the silicon nitride films, while calculating the generated second-harmonic power using the revised Maker-fringes analysis.[7] For example, in the case of a 400 nm thick SRN film (n = 2.25 at λ_{pump} = 800 nm), a relatively high dispersion of up to 10^{-2} in linear refractive index from the pump to the second-harmonic wavelength (λ_{SHG} = 400 nm) would cause a change of only 0.04% in the calculated second-harmonic power and hence dispersion in linear refractive index can be neglected. Additionally, it should be noted that the measurement errors in this study originate mainly from the fluctuation of laser power due to the unstable humidity of environment (±5%), fluctuation of readings from photomultiplier tube (PMT) resulting from the influence of background noises (±20%), and the non-uniformity in the thickness of the deposited thin films (±10%). Besides, the possibility of counting error (±10%) of photons in the PMT (Hamamatsu, Inc., H11461-03) due to pulse-overlapping, as described in the handbook, is also taken into account.[13] Furthermore, in order to minimize these errors, the generated SHG intensities from quartz and SiN thin films are determined by the average of five different spots on each sample. The revised Maker fringes analysis was then employed to carry out the tensorial analysis of the second-order nonlinearity.[7,11–13] As is evident from the figure, the generated second-harmonic signal from the film with the highest silicon content (S_3) is up to 10 times larger compared to that generated from the film with a stoichiometric composition (S_1). Additionally, these polarization dependent second-harmonic responses were then used to extract the tensorial components of the observed $\chi^{(2)}$ in these films. The extracted values of the all-normal ($\chi^{(2)}_{zzz}$) and in-plane ($\chi^{(2)}_{zxx}$) components are tabulated in Table I and are found to be up to 3.3 times larger for the SRN film (sample S_3) when compared with the stoichiometric film (sample S_1). Furthermore, to the best of our knowledge, the measured tensor component $\chi^{(2)}_{zzz}$ in the SRN film is the largest reported to-date in as-deposited PECVD silicon nitride films, and the experimental results also verify that the increasing silicon content in SiN thin films leads to enhancement in the second order nonlinear susceptibility.

ELECTRIC FIELD INDUCED ENHANCEMENT IN NONLINEARITIES

An alternative method to enhance the nonlinear response in these films is the electric-field induced second-harmonic (EFISH) effect. In our previous work,[7] we presented in-waveguide results demonstrating enhancement of the second-harmonic response from silicon nitride waveguides by applying an electric field across them. It was shown then that the applied external electric field interacts with the third-order nonlinearity of the films, resulting in a higher effective second-order response and a corresponding increase in the intensity of the second-harmonic signal from the waveguides.[7] To analyze the tunability of the nonlinear response in the SRN films, we fabricated 50 nm thick films of the three silicon nitride films sandwiched between two electrodes made of 10 nm thick layers of indium tin oxide (ITO) on a fused silicon substrate, as shown in the schematic in Fig. 2(a). The ITO films serve as the transparent electrodes across which an external DC voltage is applied while carrying out SHG experiments. It should be noted that while the ITO films were not optimized with respect to their conductance, they were still sufficient for carrying out preliminary studies on the EFISH induced tunability in the films. Figure 2(b) shows the SHG response for the SRN film, with pump and second-harmonic wavelengths of 800 and 400 nm, respectively, as a function of the applied

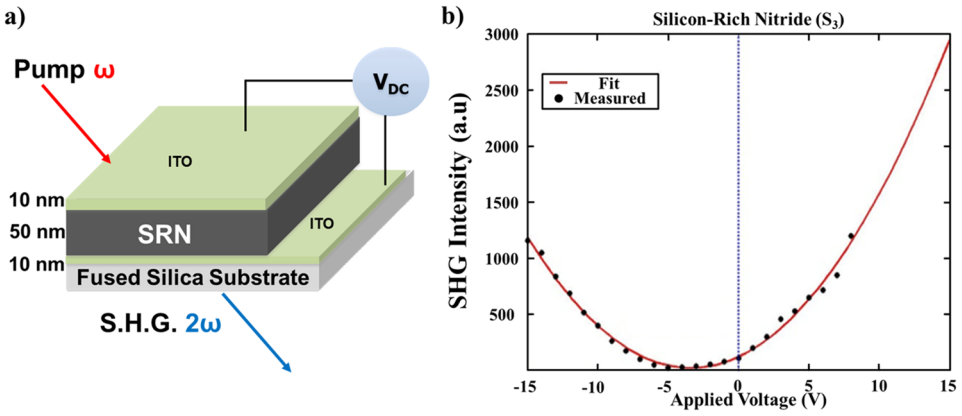

FIG. 2. (a) Schematic illustration of the SHG response (λ_{pump} = 800 nm, λ_{SHG} = 400 nm) from a 50 nm silicon nitride film sandwiched between two 10 nm ITO films on a fused silica substrate. (b) Experimental (black dots) and quadratic fitting (red) curve showing the SHG response from a SRN sample as a function of the external voltage applied across the layer.

TABLE II. As-deposited, lowest and highest effective $\chi^{(2)}$ of three different silicon nitride films with different silicon contents. The highest range of tunability is exhibited by the SRN film with a value of $\chi^{(2)}$ as high as 22.7 pm/V.

Sample	SiH_4 flow rate (sccm)	$\chi^{(2)}_{eff}$ (no bias) (pm/V)	Lowest $\chi^{(2)}_{eff}$ (pm/V)	Highest $\chi^{(2)}_{eff}$ (pm/V)
S_1*	180	2.6	2.1	3.9
S_2*	276	3.35	2.39	5.93
S_3*	500	7.5	3.9	22.7

voltage, clearly demonstrating a wide range of tunability. The SHG response is found to increase quadratically with respect to the applied voltage, which is in agreement with our prediction of EFISH. It should also be noted that the minimum in the measured quadratic response is found to be at a small negative bias voltage and not at zero-bias. This is because at this voltage, the artificially created second-order nonlinearity generated by the external electric field and the high $\chi^{(3)}$ coefficient of SiN perfectly negates the all-normal $\chi^{(2)}_{zzz}$ present in the as-deposited film. As a result, the magnitude of the SHG response reduces but is still not perfectly zero because of contributions from the in-plane components of the $\chi^{(2)}$ in the as-deposited nitride film, ITO layers, as well as those arising out of any surface nonlinearities.

The SHG signal measured at an applied voltage of 8 V was found to be up to 36 times larger than that measured at zero-bias. Table II summarizes the calculated highest and lowest effective $\chi^{(2)}_{zzz}$ components of three different silicon nitride samples fabricated with the same silicon contents as S_1, S_2, and S_3. The SRN film demonstrates an effective $\chi^{(2)}$ spanning from ~3 pm/V to as high as 22 pm/V. This relatively large range of tunability is in accordance with reports in the literature of an enhanced third-order nonlinear response in silicon-rich nitride films when compared to their stoichiometric counterparts[14–16]

DISPERSION IN THE OBSERVED NONLINEARITY

The bulk of the studies on second-order nonlinearities in silicon nitride films have been carried out using either 800 nm or 1064 nm sources.[6,11] While the values of nonlinearities reported using these pump wavelengths are relatively high, other studies which pursue in-waveguide experiments at a pump wavelength of 1550 nm have measured lower values of the nonlinearity.[7,8] The cause of this discrepancy between values measured using two different pump-wavelengths was attributed previously to a lack of perfect phase-matching in waveguide SHG experiments carried out using a pump at 1550 nm.

To test for wavelength dependence in the nonlinearities of our films, we carried out reflection SHG measurements on all three samples, using pumps at 1040 nm and 1550 nm. These two wavelengths were chosen solely based on source availability. The exact methodology employed in carrying out these measurements is detailed in the supplementary material, while the optical setup is shown in Fig. 3(a). To make a fair comparison, parameters such as an incident angle, spot size of the beam, average pump power, and polarization state were kept constant while carrying out the measurements across the three samples. Figure 3(b) shows the magnitude of the SHG signal, corresponding to the polarization with the maximum second-harmonic signal, generated from the three samples at the two pump-wavelengths. Sample S_3, with the highest silicon content, demonstrates the largest second-harmonic signal among the three samples at both pump wavelengths.

Dispersion in nonlinear susceptibilities is a well-known phenomenon explained by Miller's rule, which defines a relation between dispersion in refractive index and dispersion in second-order nonlinearities.[18,19] Furthermore, work in the literature has shown a correlation between increasing silicon content in silicon nitride films and the dispersion in refractive index of such films.[11] These two facts together imply that dispersion in $\chi^{(2)}$ is expected from 1040 nm to 1550 nm and expected to be the highest in the film with the highest silicon content. However, the magnitude of dispersion demonstrated in this work far exceeds that predicted by Miller's rule and therefore the exact origins of this remains to be explained. Specifically, a difference in magnitude of second harmonic generation between 1040 nm and 1550 nm of 41, 42, and 39 times is seen across the three films S_3, S_2, and S_1, respectively. Since the power in the second-harmonic signal is proportional to the square of the second-order nonlinear coefficient, this

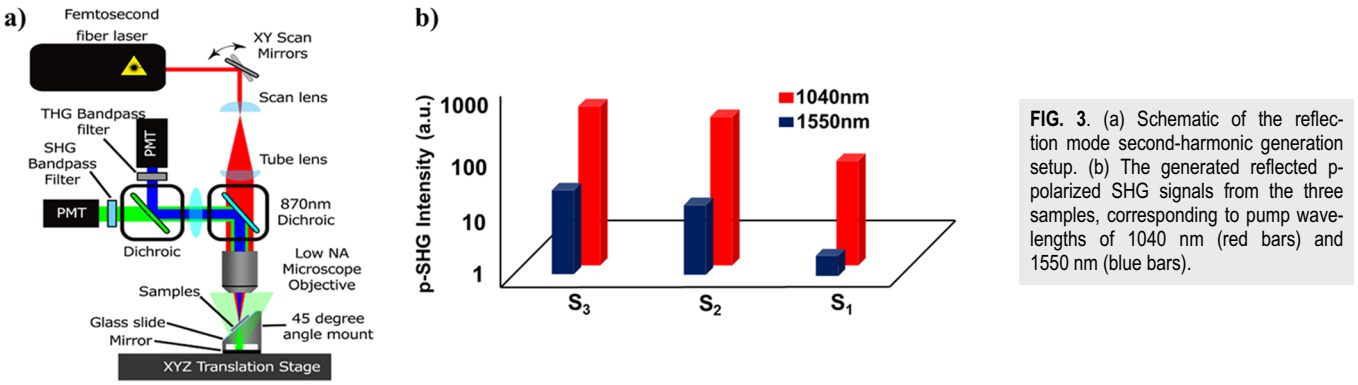

FIG. 3. (a) Schematic of the reflection mode second-harmonic generation setup. (b) The generated reflected p-polarized SHG signals from the three samples, corresponding to pump wavelengths of 1040 nm (red bars) and 1550 nm (blue bars).

implies that the effective $\chi^{(2)}$ value measured using a 1550 nm pump is smaller by up to ~6.4 times than that measured using a 1040 nm pump.

IN-WAVEGUIDE LOSS CHARACTERIZATIONS

To characterize the viability of SRN films for on-chip applications, in-waveguide loss measurements were carried out using SRN waveguides on oxide-on-silicon substrates. The thicknesses of the SRN device layer, deposited using PECVD, and that of the oxide below were 430 nm and 3 μm, respectively. Ring-resonators coupled to bus waveguides were then fabricated using a combination of electron beam lithography and inductively coupled plasma reactive ion etching (ICP-RIE) using a C_4F_8, SF_6 plasma, as outlined in Ref. 7. The waveguide widths were kept at 1000 nm, and the coupling gaps were varied from 150 to 300 nm, in the case of TE_0, and from 500 to 700 nm, in the case of TM_0 transmission to achieve critical coupling. The choice of the width and height was made keeping in mind the need to have single-mode operation of both TE- and TM-polarized modes at a wavelength of 1550 nm. In-waveguide measurements were then performed using a fiber-in, free-space out setup with an Agilent 8164-B tunable CW laser source spanning a wavelength range of 1.46 to 1.64 μm.[7,17] Figure 4 shows the measured normalized transmission (dB) of the ring-resonators for TE and TM polarizations for the cases closest to the critical coupling regime. This was achieved in the case of TE transmission at a coupling gap of 250 nm and at a gap of 600 nm for TM transmission.

The propagation loss values for the TE and TM cases, calculated from resonances at 1524.7 nm and 1563.9 nm, were found to be 9.54 and 14.60 dB/cm, respectively.[17] These values, while relatively high when compared to stoichiometric silicon nitride waveguides, are close to other in-waveguide loss measurements for SRN films in the literature.[14] Furthermore, these can be improved by optimizing the fabrication process such as the etching recipe and/or employing post-deposition annealing, as well as by increasing the width of the waveguide to reduce sidewall scattering.[7] It should also be noted that the reason for the higher propagation loss observed in the TM case is likely due to the lower confinement of the optical mode in the waveguide core leading to a higher interaction with the top-cladding oxide. Thick PECVD oxides deposited on waveguide structures are known to have imperfections and air voids leading to higher scattering loss for the propagating modes.[7] Finally, while the results presented here are for the linear losses in the SRN waveguides, they are expected to exhibit negligible nonlinear losses, such as those due to two photon absorption (TPA). This is discussed extensively in the work by Ooi *et al.*,[16] where it is shown that TPA only becomes a dominant loss mechanism in SRN films exceeding a refractive index of 3.

CONCLUSIONS AND DISCUSSION

Historically, bulk second-order nonlinearities in silicon nitride films have been an anomalous finding, and as such, their exact origins have been ambiguous. Furthermore, the variety of techniques employed to deposit and characterize these films leads to further confusion in the reported properties of such films. It is therefore important to make a fair comparison of these films in terms of deposition technique, wavelength of characterization, and silicon content.

In our past work, we have reported a large discrepancy of up to an order of magnitude in the nonlinear coefficient of stoichiometric nitride films. These were extracted in free-space at 800 nm and in-waveguide at 1550 nm, using phase-matched SHG. In this case, we hypothesized that the discrepancy was due to a lack of perfect phase-matching and/or material changes due to processing during waveguide fabrication.[7] Similarly, recent independent results by Billat *et al.* and Porcel *et al.*[8,20] demonstrated all-optical quasi-phase matched SHG in stoichiometric silicon nitride waveguides, reporting a value of 0.3 pm/V (at 1550 nm) and 3.7 pm/V (at 1064 nm), respectively. These results achieved quasi-phase matching due to an all-optical, charge separation-induced grating in the silicon nitride waveguides, via the coherent photogalvanic effect (CPE). The latter study attributes the higher coefficient observed to the nature of the nitride film deposited and compares these results to other reported coefficients including those in Ref. 7. However, care was not taken to account for the wavelength employed in each of the studies to which the authors compare their result. Considering the results in our current study, we attribute the large discrepancy in these references to the dispersion in the nonlinearity of stoichiometric nitride thin films as opposed to an inherently larger coefficient. This observed dispersion, it

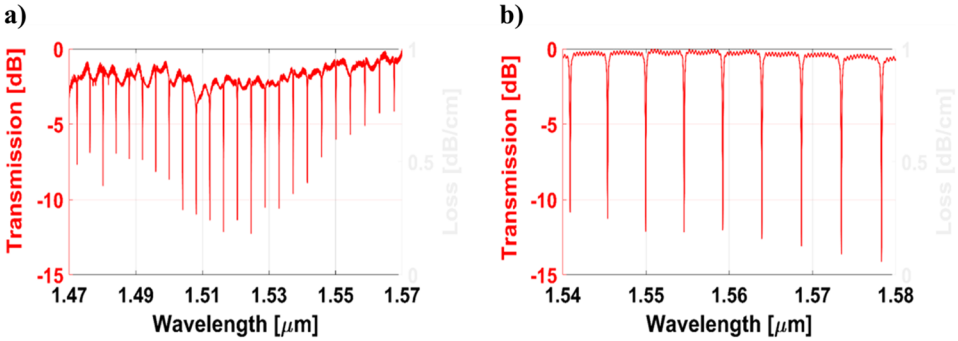

FIG. 4. (a) Normalized transmission, across a wavelength range of 1.47–1.57 μm, of the TE_0 mode in a 1 μm wide SRN waveguide coupled to a ring-resonator at a coupling gap of 250 nm.[17] (b) Normalized transmission, across a wavelength range of 1.54–1.58 μm, of the TM_0 mode in a 1 μm wide SRN waveguide coupled to a ring-resonator at a coupling gap of 600 nm.

should be noted, is much higher than what can be attributed to Miller's rule,[18] which relates the relative magnitude of the nonlinear susceptibilities to the linear susceptibilities at the respective wavelengths. The exact origin of this high dispersion remains to be explained. Finally, this study's use of thin-films was carefully chosen to be performed in free space to avoid the need for phase matching of any kind, neither all optical quasi-phase matching nor modal dispersion-based phase matching.

In summary, this work has clearly demonstrated that increasing silicon content in PECVD deposited silicon nitride films results in enhancement in the second-order nonlinearity of such films, achieving a value as high as 8 pm/V in as-deposited SRN films. We then demonstrate a relatively large tunability range of the nonlinear coefficient, with a highest demonstrable coefficient of 22 pm/V. Furthermore, we demonstrate that the inherent nonlinearity in as-deposited films is highly dispersive, not just in the case of silicon-rich compositions but also in the case of stoichiometric films. Finally, it is our opinion that the highly dispersive nature of the second-order nonlinearity in these films should be taken into consideration by any future studies comparing the nonlinearity and/or evaluating the viability of such films for on-chip nonlinear and or electro-optic applications.

SUPPLEMENTARY MATERIAL

A brief description of the optical characterization setups employed to carry out both the maker fringes analysis and the dispersion studies of the second order nonlinear susceptibility are included in the supplementary material.

ACKNOWLEDGMENTS

This work was supported by the Defense Advanced Research Projects Agency (DARPA), the National Science Foundation (NSF), the NSF ERC CIAN, NSF's NNCI San Diego Nanotechnology Infrastructure (SDNI), the NSF Graduate Research Fellowship under No. DGE-1143953, the Office of Naval Research (ONR) Multidisciplinary University Research Initiative (MURI), the Army Research Office (ARO), and the Cymer Corporation. We thank UCSD's staff Ryan Anderson for the discussion on the equipment for electrical characterization.

REFERENCES

[1]C. Malgrange, C. Ricolleau, and M. Schlenker, *Symmetry and Physical Properties of Crystals* (Springer, 2014).
[2]R. S. Jacobsen, K. N. Andersen, P. I. Borel, J. Fage-Pedersen, L. H. Frandsen, O. Hansen, A. V. Martin Kristensen Lavrinenko, G. Moulin, H. Ou, and C. Peucheret, Nature **441**(7090), 199 (2006).
[3]M. Cazzanelli, F. Bianco, E. Borga, G. Pucker, M. Ghulinyan, E. Degoli, E. Luppi, V. Véniard, S. Ossicini, D. Modotto, and S. Wabnitz, Nat. Mater. **11**(2), 148 (2012).
[4]D. J. Moss, R. Morandotti, A. L. Gaeta, and M. Lipson, Nat. Photonics **7**(8), 597 (2013).
[5]J. S. Levy, M. A. Foster, A. L. Gaeta, and M. Lipson, Opt. Express **19**(12), 11415–11421 (2011).
[6]T. Ning, H. Pietarinen, O. Hyvarinen, J. Simonen, G. Genty, and M. Kauranen, Appl. Phys. Lett. **100**, 161902 (2012).
[7]M. W. Puckett, R. Sharma, H. Lin, M. Yang, F. Vallini, and Y. Fainman, Opt. Express **24**, 16923 (2016).
[8]A. Billat, D. Grassani, M. HP Pfeiffer, S. Kharitonov, T. J. Kippenberg, and B. Camille-Sophie, Nat. Commun. **8**(1), 1016 (2017).
[9]A. Kitao, K. Imakita, I. Kawamura, and M. Fujii, J. Phys. D: Appl. Phys. **47**, 215101 (2014).
[10]H. Lin, R. Sharma, M. Yang, M. W. Puckett, C. D. Wurm, F. Vallini, and Y. Fainman, in *CLEO: Science and Innovations* (Optical Society of America, 2017), pp. SM1M–6.
[11]K. Koskinen, R. Czaplicki, A. Slablab, T. Ning, A. Hermans, B. Kuyken, V. Mittal, G. S. Murugan, T. Niemi, R. Baets, and M. Kauranen, Opt. Lett. **42**(23), 5030–5033 (2017).
[12]H. Lin, M. Yang, R. Sharma, M. W. Puckett, S. Montoya, C. D. Wurm, F. Vallini, E. E. Fullerton, and Y. Fainman, Appl. Phys. Lett. **110**, 113103 (2017).
[13]H. Lin, F. Vallini, M. Yang, R. Sharma, M. W. Puckett, S. Montoya, C. D. Wurm, E. E. Fullerton, and Y. Fainman, Sci. Rep. **7**, 9983 (2017).
[14]J. W. Choi, G. F. R. Chen, D. K. T. Ng, K. J. A. Ooi, and D. T. H. Tan, Sci. Rep. **6**, 27120 (2016).
[15]C. Lacava, S. Stankovic, A. Z. Khokhar, T. D. Bucio, F. Y. Gardes, G. T. Reed, D. J. Richardson, and P. Petropoulos, Sci. Rep. **7**(1), 22 (2017).
[16]K. J. A. Ooi, D. K. T. Ng, T. Wang, A. K. L. Chee, S. K. Ng, Q. Wang, L. K. Ang, A. M. Agarwal, L. C. Kimerling, and D. T. H. Tan, Nat. Commun. **8**, 13878 (2017).
[17]R. Sharma, M. W. Puckett, H. Lin, A. Isichenko, F. Vallini, and Y. Fainman, Opt. Lett. **41**(6), 1185–1188 (2016).
[18]R. C. Miller, Appl. Phys. Lett. **5**(1), 17–19 (1964).
[19]A. Hermans, C. Kieninger, K. Koskinen, A. Wickberg, E. Solano, J. Dendooven, M. Kauranen, S. Clemmen, M. Wegener, C. Koos, and R. Baets, Sci. Rep. **7**, 44581 (2017).
[20]M. A. G. Porcel, J. Mak, C. Taballione, V. K. Schermerhorn, J. P. Epping, P. J. M. V. D. Slot, and K. J. Boller, Opt. Express **25**(26), 33143–33159 (2017).